Split ring resonator sensors for infrared detection of single molecular monolayers

Ertugrul Cubukcu,[1,a)] Shuang Zhang,[1] Yong-Shik Park,[1] Guy Bartal,[1] and Xiang Zhang[1,2,b)]
[1]*Nanoscale Science and Engineering Center, University of California, 5130 Etcheverry Hall, Berkeley, California 94720-1740, USA*
[2]*Materials Sciences Division, Lawrence Berkeley National Laboratory, 1 Cyclotron Road, Berkeley, California 94720, USA*

(Received 24 June 2009; accepted 11 July 2009; published online 31 July 2009)

We report a surface enhanced molecular detection technique with zeptomole sensitivity that relies on resonant coupling of plasmonic modes of split ring resonators and infrared vibrational modes of a self-assembled monolayer of octadecanthiol molecules. Large near-field enhancements at the gap of split ring resonators allow for this resonant coupling when the molecular absorption peaks overlap spectrally with the plasmonic resonance. Electromagnetic simulations support experimental findings. © *2009 American Institute of Physics*. [DOI: 10.1063/1.3194154]

Surface enhanced vibrational spectroscopy[1] has been a topic of interest for interdisciplinary research owing to its ability to amplify molecular scattering cross sections through localized surface plasmon resonance.[2,3] Surface enhanced Raman spectroscopy (SERS)[4–6] and surface enhanced infrared absorption spectroscopy (SEIRA)[7–9] are commonly employed techniques in which the minimum detection limit is determined by the strength of local fields around the metallic nanostructures. Various nanoparticle geometries, including nanospheres, nanorods,[6] and nanoshells,[10] have been utilized for SERS. Recently, Neubrech *et al.*[11] have introduced an approach for SEIRA that relies on Fano-like resonances due to resonant coupling between a nanorod and a molecular monolayer.

In this letter, we experimentally demonstrate optical detection of self-assembled monolayers (SAMs) (Ref. 12) of 1-octadecanthiol $[CH_3(CH_2)_{18}SH]$ through resonant coupling between plasmonic modes of split ring resonators (SRRs) and vibrational modes of 1-octadecanthiol (ODT) molecules. This resonant coupling occurs when the absorption of CH_2 stretching vibrations of ODT overlaps spectrally with the plasmonic resonance of the SRR. Figure 1(a) shows the typical setup for this sensing paradigm. A nanofabricated array of SRRs is coated with a monolayer of ODT. Absorption by molecules in the nanoscale gap modifies the SRR resonance spectrum upon interaction with the enhanced near-field in the gap [Fig. 1(b)]. This effect manifests itself in the far-field transmission spectrum allowing us to detect the ODT molecules using far-field microscopy techniques. Our approach differs from previous plasmonic sensing schemes that rely on the local index change.[13,14]

We first modeled the effect of aforementioned coupling mechanism on the SRR resonance spectrum by solving the three dimensional electromagnetic problem with a commercial finite integration technique solver (CST Microwave Studio). Figure 1(b) shows the near-field distribution of a pristine SRR without the ODT layer. Notably, the field is strongly localized and confined in the gap region.[15] The parameters used in this calculation for the gold SRR array are the following: period $a=800$ nm, radius $r=200$ nm, thickness $t=30$ nm, width $w=80$ nm, and gap $g=30$ nm. Having calculated the near-field distribution for the pristine SRRs, the SRR surfaces are uniformly covered with a 2.4 nm thick layer characterized with a Lorentz oscillator model to emulate the effect of the ODT molecules on the SRR spectrum both in the near and the far zones. The parameters for the Lorentz oscillator are chosen such that they can reproduce the absorption associated with the symmetric stretching mode of the ODT molecule.

The SRR-molecule coupling results in a dip in the near-field spectrum of the SRR, as shown in Fig. 2(a). The presence of the ODT on the SRR is essentially equivalent to local absorption at the vibrational frequency of ODT for the SRR. From the ODT point of view, there is more available energy to be absorbed as the SRR confines and enhances the incoming radiation in the gap similar to impedance matching in electronic circuits. In other words, the ODT absorption cross section is increased by the SRR antenna cross section.

In the far field, however, there is a peak at the ODT absorption frequency in the SRR forward scattering (transmission) spectrum in the presence of the ODT layer. The energy absorbed by the ODT molecules in the near-field couples back to the SRR through Rayleigh scattering and is radiated by the SRR antenna. During this reradiation process, the part of the electromagnetic energy, which would nor-

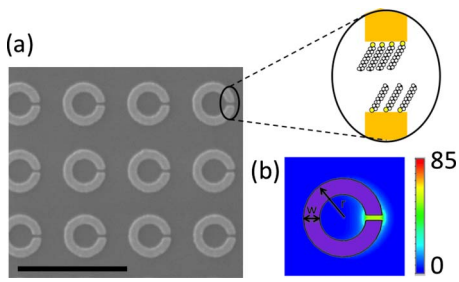

FIG. 1. (Color online) (a) Scanning electron micrograph of a typical SRR array. Scale bar is 1 μm. Inset shows a schematic of a SAM of ODT molecules in the gap of a single SRR for absorption spectroscopy. (b) Simulated near-field amplitude distribution around a SRR on resonance for polarization along the gap. Near-field is confined mostly in the gap.

a)Electronic mail: cubukcu@berkeley.edu.
b)Author to whom correspondence should be addressed. Electronic mail: xzhang@me.berkeley.edu.

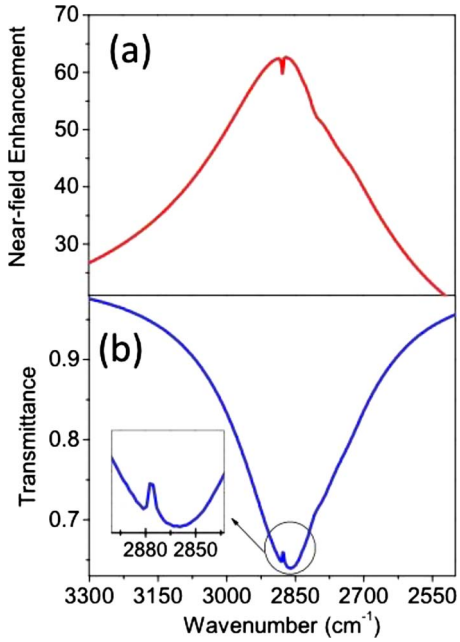

FIG. 2. (Color online) (a) Calculated near-field spectrum in the SRR gap with a uniform 2.4 nm layer of a Lorentzian absorber on SRRs to emulate the experiments. (b) Calculated far-field transmission spectrum for the same configuration. Inset is a closer view of the molecular absorption peak superimposed on the SRR spectrum.

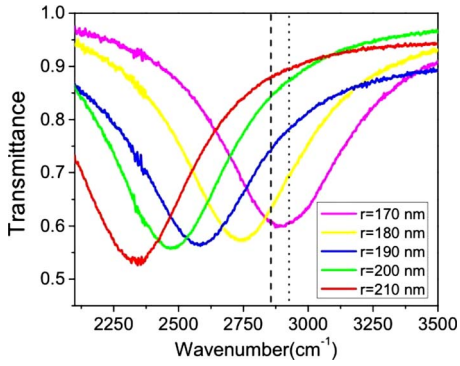

FIG. 3. (Color online) Measured transmittance for five SRR arrays with different diameters for polarization along the gap. Vertical lines represent the position of ODT absorption peaks relative to different SRR spectra.

mally not scatter in the forward direction is radiated in the forward direction due to the SRR-ODT near-field coupling.

To demonstrate this coupling mechanism we have fabricated five different SRR arrays with radius 170, 180, 190, 200, and 210 nm. The other array parameters were same as those used in the simulations except for the period $a=600$ nm. The SRR arrays were fabricated on an indium tin oxide coated quartz substrate by standard electron beam lithography with a single PMMA (poly-methyl-methacrylate) layer followed by a lift-off process [Fig. 1(a)]. Each array consists of 2500 SRRs corresponding to an area of 30×30 μm^2. Infrared (IR) transmission measurements are performed on a Fourier transform IR (FTIR) spectrometer equipped with a microscope. The mid-IR illumination is focused on to the samples with a $36\times$ 0.5 numerical aperture Cassegrain reflective objective and the transmitted signal is collected with another microscope objective of same specifications on to a liquid nitrogen cooled mercury-cadmium-telluride detector. The sample area of interest is spatially filtered with an adjustable square aperture in the microscope beam path to limit the transmitted signal to the 30×30 μm^2 area of the SRR arrays. The illumination was unpolarized whereas the collection path polarizer was aligned along the gap of the SRRs. Each spectrum is normalized to the spectrum of transmitted signal through a nearby part of the sample that does not have any SRRs so as to correct for the spectrum of the IR radiation source.

The SRR acts like a resistive-capacitive-inductive (*RLC*) resonant optical circuit.[16] In general, they are of interest for their artificial magnetic properties in applications such as negative refraction.[17–20] Here we are interested in their ability to enhance electric fields in the near zone. Essentially, SRRs are optical antennas[21–23] with a small footprint owing to their compact geometry compared to their linear optical antenna counterparts. The SRR resonance occurs when the perimeter of the SRR loop is a half integer multiple of the wavelength of optical current circulating in the metal. Therefore the SRR antenna resonance can be tuned by changing the radius and in turn the perimeter of the SRR. The other advantage of using SRRs as opposed to regular nanorod antennas is that SRRs naturally have a gap offering potentially larger near-field enhancements, which will in turn increase sensitivity. By introducing smaller gaps within the nanofabrication limits, the sensitivity can be further improved.

The transmission resonance of the five different SRR arrays fabricated with different radii cover wavenumbers in the range 2250–3000 cm^{-1} (Fig. 3). Each IR spectrum is an average of 50 different spectral scans with a 2 cm^{-1} resolution. By changing the radius of the SRRs, the plasmonic resonance can be tuned to allow for spectral overlap between SRR resonance and the ODT absorption spectrum. The SRR array resonance for 170 nm radius overlaps well with both symmetric and antisymmetric stretching vibrational modes of the ODT molecule.

Having characterized the plasmonic resonance spectra of these pristine SRR arrays, we covered them with a monolayer of the ODT molecule. The samples were immersed in a 2.5 mM solution of ODT (Sigma-Aldrich, 98%) in ethanol (Sigma-Aldrich; anhydrous, 99%) for 3 h. The deposition process is performed at room temperature. In order to remove the excess reactants the samples are then ultrasonically rinsed in ethanol and dried with nitrogen gas. The long ODT molecules form a 2.4 nm thick monolayer with their thiol headgroup chemisorbed on the gold surface. The molecular axis is slightly tilted with respect to the gold surface normal.

The IR transmission measurements are performed on SRR arrays coated with the ODT monolayer using an FTIR microspectroscopy setup as described above. The IR spectra for SRR arrays are shown in Fig. 4(a). The symmetric (2850–2863 cm^{-1}) and antisymmetric (2916–2936 cm^{-1}) C–H stretching vibrational modes are manifested in the far-field SRR spectra allowing for the detection and the identification of the ODT molecules when the SRR resonance overlaps with the ODT absorption as in the case of 170 and 180 nm radii. When the SRR resonance is detuned by changing the SRR radius from the ODT absorption, the vibrational stretching modes are hardly discernable in the IR spectrum. This resonant electromagnetic coupling mechanism is reminiscent of Fano resonances that originate from quantum mechanical interaction of a discrete state with a continuum of states.[11,24]

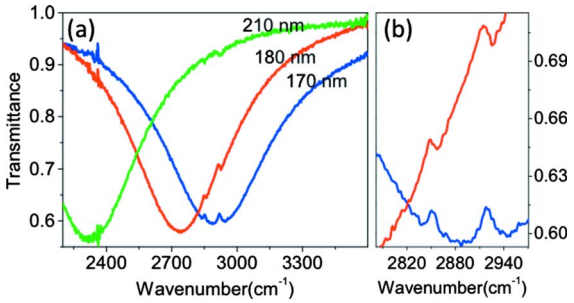

FIG. 4. (Color online) (a) Measured transmittance spectra for three different SRR arrays with radii 170 nm (blue), 180 nm (red), and 210 nm (green) with the SAM. Two peaks corresponding to ODT absorption are clearly visible. (b) Closeup view of the resonance region in (a).

For the case of strongest resonant coupling (r=170 nm), the contrast between the maximum and the minimum transmittance at the antisymmetric vibrational frequency is about 1.9%. This contrast is a function of both the near-field enhancement and the number of molecules adsorbed on the gold surface. Since the current approach relies on the molecular self-assembly process, signal contrast is limited by a monolayer for a given near-field enhancement. Although this technique has single monolayer sensitivity, signal to noise ratio is essentially limited by the surface area of the region of highest near-field enhancement. Based on the surface packing density of the ODT molecules of 22.2 $Å^2$/molecule and the gap surface area of a single SRR of $2\times30\times80$ nm^2, there are about 22 000 molecules corresponding to $\approx$40 zeptomoles per SRR. Here the only assumption is that the ODT signal originates primarily from the gap region where the near-field is strongly confined.

In summary, we demonstrate a plasmonic detection technique that relies on the resonant electromagnetic coupling between a SRR and the IR vibrational modes of molecules. This technique's ability to provide spectral fingerprint information along with its extremely low detection limit offer many possibilities in future IR vibrational spectroscopy on the nanoscale.

We acknowledge financial support from the National Institutes of Health through the NIH Roadmap for Medical Research (PN2 EY018228) and the NSF Nanoscale Science and Engineering Center (NSEC) under Grant No. CMMI-0751621.

[1]R. Aroca, *Surface Enhanced Vibrational Spectroscopy* (Wiley, Hoboken, NJ, 2006).
[2]H. Raether, *Surface Plasmons on Smooth and Rough Surfaces and on Gratings* (Springer, Berlin, 1986).
[3]E. Ozbay, Science **311**, 189 (2006).
[4]A. Campion and P. Kambhampati, Chem. Soc. Rev. **27**, 241 (1998).
[5]M. Moskovits, Rev. Mod. Phys. **57**, 783 (1985).
[6]S. M. Nie and S. R. Emery, Science **275**, 1102 (1997).
[7]J. Kundu, F. Le, P. Nordlander, and N. J. Halas, Chem. Phys. Lett. **452**, 115 (2008).
[8]D. Enders and A. Pucci, Appl. Phys. Lett. **88**, 184104 (2006).
[9]T. R. Jensen, R. P. Van Duyne, S. A. Johnson, and V. A. Maroni, Appl. Spectrosc. **54**, 371 (2000).
[10]F. Le, D. W. Brandl, Y. A. Urzhumov, H. Wang, J. Kundu, N. J. Halas, J. Aizpurua, and P. Nordlander, ACS Nano **2**, 707 (2008).
[11]F. Neubrech, A. Pucci, T. W. Cornelius, S. Karim, A. Garcia-Etxarri, and J. Aizpurua, Phys. Rev. Lett. **101**, 157403 (2008).
[12]F. Schreiber, Prog. Surf. Sci. **65**, 151 (2000).
[13]A. D. McFarland and R. P. Van Duyne, Nano Lett. **3**, 1057 (2003).
[14]B. Lahiri, A. Z. Khokhar, R. M. De La Rue, S. G. McMeekin, and N. P. Johnson, Opt. Express **17**, 1107 (2009).
[15]K. Aydin, A. O. Cakmak, L. Sahin, Z. Li, F. Bilotti, L. Vegni, and E. Ozbay, Phys. Rev. Lett. **102**, 013904 (2009).
[16]A. Alu and N. Engheta, Phys. Rev. Lett. **101**, 043901 (2008).
[17]T. J. Yen, W. J. Padilla, N. Fang, D. C. Vier, D. R. Smith, J. B. Pendry, D. N. Basov, and X. Zhang, Science **303**, 1494 (2004).
[18]J. B. Pendry, A. J. Holden, D. J. Robbins, and W. J. Stewart, IEEE Trans. Microwave Theory Tech. **47**, 2075 (1999).
[19]K. Aydin, K. Guven, M. Kafesaki, L. Zhang, C. M. Soukoulis, and E. Ozbay, Opt. Lett. **29**, 2623 (2004).
[20]I. Bulu, H. Caglayan, K. Aydin, and E. Ozbay, New J. Phys. **7**, 223 (2005).
[21]P. Muhlschlegel, H. J. Eisler, O. J. F. Martin, B. Hecht, and D. W. Pohl, Science **308**, 1607 (2005).
[22]E. Cubukcu, E. A. Kort, K. B. Crozier, and F. Capasso, Appl. Phys. Lett. **89**, 093120 (2006).
[23]E. Cubukcu, N. F. Yu, E. J. Smythe, L. Diehl, K. B. Crozier, and F. Capasso, IEEE J. Sel. Top. Quantum Electron. **14**, 1448 (2008).
[24]U. Fano, Phys. Rev. **124**, 1866 (1961).